[13] Martorella, M.
A novel approach for ISAR image cross-range scaling.
IEEE Transactions on Aerospace and Electronic Systems, **44**, 1 (2008), 281–294.

[14] Yeh, C-M., et al.
Cross-range scaling for ISAR based on image rotation correlation.
IEEE Geoscience and Remote Sensing Letters, **6**, 3 (2009), 597–601.

[15] Munoz-Ferreras, J. and Perez-Martinez, F.
Pitch estimation for non-cooperative maritime targets in ISAR scenarios.
IET Radar, Sonar & Navigation, **3**, 5 (2009), 521–529.

[16] Gaffar, M., Nel, W., and Inggs, M.
Selecting suitable coherent processing time window lengths for ground-based ISAR imaging of cooperative sea vessels.
IEEE Transactions on Geoscience and Remote Sensing, **47** (Sept. 2009), 3231–3240.

[17] Martorella, M. and Berizzi, F.
Time windowing for highly focused ISAR image reconstruction.
IEEE Transactions on Aerospace and Electronic Systems, **41** (2005), 992–1007.

[18] Pastina, D. and Spina, C.
Slope-based frame selection and scaling technique for ship ISAR imaging.
IET Signal Processing, **2**, 3 (2008), 265–276.

[19] Ward, K., Tough, R., and Haywood, B.
Hybrid SAR-ISAR imaging of ships.
Record of the IEEE 1990 International Radar Conference, Arlington, VA, May 7–10, 1990, pp. 64–69.

[20] Berizzi, F.
ISAR imaging of targets at low elevation angles.
IEEE Transactions on Aerospace and Electronic Systems, **37** (Apr. 2001), 419–435.

[21] Palmer, J., et al.
ISAR imaging using an emulated multistatic radar system.
IEEE Transactions on Aerospace and Electronic Systems, **41**, 4 (2005), 1464–1472.

[22] Martorella, M., et al.
Optimal sensor placement for multi-bistatic ISAR imaging.
Proceedings of the 2010 European Radar Conference (EuRAD), Paris, Sept. 30–Oct. 1, 2010, pp. 228–231.

Range-Doppler Resolution of the Linear-FM Noise Radar Waveform

This research considers the linear-FM (LFM) of a noise radar waveform for resolving targets when channel noise and four popular radar sidelobe weighting functions are considered. By using large time-bandwidth products and systematically varying the phase scaling factor κ, results from the digital matched filter output provide evidence that the LFM noise waveform 1) has range-Doppler resolution similar to conventional chirp waveforms and 2) has a low probability of intercept (LPI) similar to random noise waveforms. We acquire the results using a computer-based simulation and verify the location of target peaks using the chirp waveform output for both stationary and moving target cases.

I. INTRODUCTION

The chirp waveform serves as the preferred radar waveform because the resultant time-bandwidth product is much larger than unity [1]. By using digital signal processing, a large bandwidth β is realized without having to transmit an extremely short pulse duration τ. The idea of realizing large bandwidths with even larger pulse durations results in a pulse compression gain defined by the time-bandwidth product. Furthermore, the matched filter process achieves correlation with target returns that have Doppler shifts $\neq 0$. As a result the chirp waveform is said be "Doppler tolerant" despite the subsequent range measurement error $\delta R = -cf_D/2\mu$, where c is the speed of light, f_D is the Doppler frequency, and μ is the chirp rate.

The use of random noise and/or random signals for radar-based applications has been pursued by several research institutions [2–8]. One of the main appeals behind these types of radar waveforms is that they are inherently immune to cochannel interference (CCI) [9, 10]. In theory the random noise waveform produces a "thumbtack" radar ambiguity function with a single central peak and no energy in the range-Doppler plane [11]. The central peak suggests excellent range and Doppler resolution, but very poor Doppler tolerance. As a result the receive process for the random noise waveform must be set to a specific delay and, therefore, would be limited for a practical moving target indication (MTI) application [12].

Manuscript received August 18, 2011; revised January 4, 2012; released for publication July 3, 2012.

IEEE Log No. T-AES/49/1/944380.

Refereeing of this contribution was handled by R. Narayanan.

The purpose of this paper is to demonstrate how linear FM (LFM) and the phase scaling factor enable the random noise waveform to serve as a suitable MTI waveform for both stationary and moving targets in the presence of channel noise. The phase scaling factor plays a critical role in ensuring that the resulting waveform is optimized for the radar application. We analyze the matched filter output for an LFM noise radar waveform when non-zero, Doppler-shifted delays are considered. In Section II we define the signal set and evaluate the ambiguity function of the LFM noise waveform. We briefly discuss some of the ambiguity function characteristics and draw comparisons to the chirp and random noise waveforms. In Section III we analyze the matched filter output and demonstrate the range-Doppler resolution of the LFM noise waveform. We conclude that the LFM noise waveform offers advantages over the random noise waveform and performs comparable with the conventional chirp waveform.

II. LINEAR-FM OF NOISE RADAR WAVEFORM

The baseband, discrete-time equivalent of the complex chirp is defined as

$$s[n] = e^{j\pi\mu n^2} \qquad \text{for} \quad -N \le n \le N \tag{1}$$

where μ is the chirp rate, $n = t/T_s$ is the discrete-time index, $T_s = \tau/N$ is the sampling period with pulse duration τ, and $s[n]$ is one of $N = 2^{\lceil \log_2(\tau\beta) \rceil}$ time samples. By discretizing the chirp and appreciating the fact that it has constant envelope with quadratic phase, we can conveniently represent (1) using vector notation as

$$\mathbf{s} = \begin{bmatrix} e^{j\pi\mu N^2} \\ e^{j\pi\mu(-N+1)^2} \\ \vdots \\ e^{j\pi\mu(N-1)^2} \\ e^{j\pi\mu N^2} \end{bmatrix}. \tag{2}$$

The noise waveform is also defined using vector notation and has Rayleigh-distributed amplitude and uniformly-distributed phase $\mathcal{U}(0, 2\pi)$. The phase is even by design. This ensures that the matched filter process is successfully realized using Fourier symmetry properties. We represent the amplitude $\mathbf{a}$ and phase $\mathbf{p}$ of the LFM noise waveform as

$$\mathbf{a} = \begin{bmatrix} a_{-N} \\ a_{-N+1} \\ \vdots \\ a_{N-1} \\ a_N \end{bmatrix}, \qquad \mathbf{p} = \begin{bmatrix} e^{j\kappa p_{-N}} \\ e^{j\kappa p_{-N+1}} \\ \vdots \\ e^{j\kappa p_{N-1}} \\ e^{j\kappa p_N} \end{bmatrix} \tag{3}$$

where κ is a phase scaling factor discussed shortly. By imposing LFM on the noise waveform, we can define the transmit waveform as

$$\mathbf{v} = \mathbf{a} \circ \mathbf{p} \circ \mathbf{s} = \begin{bmatrix} a_{-N} \exp[j(\kappa p_{-N} + \pi\mu N^2)] \\ a_{-N+1} \exp[j(\kappa p_{-N+1} + \pi\mu(-N+1)^2)] \\ \vdots \\ a_{N-1} \exp[j(\kappa p_{N-1} + \pi\mu(N-1)^2)] \\ a_N \exp[j(\kappa p_N + \pi\mu N^2)] \end{bmatrix} \tag{4}$$

where $(\circ)$ represents the Hadamard (element-wise) product.

Next, we consider a point target of arbitrary reflectivity ζ, whose radar cross section (RCS) is constant over time and frequency and is moving with radial velocity v relative to the radar. The resultant delay is $d = t_0 - (2v/c)t$, where t_0 is the target initial delay, v is the radial velocity, c is the speed of light, and t is continuous-time. After discretization of the receive signal, the target delay d will correspond to a discrete-time sample that will, most likely, not be an integer value. A quantizer implements the rounding operation, but in doing so, it causes a range measurement error since the precision of the quantizer is limited. The receive signal plus noise $x[n] = \zeta \cdot v[n-\eta] + \epsilon$, where $\eta = d/T_s$ is rounded to the nearest integer such that $\eta \in \mathcal{Z}[-N, N]$. The receive signal can be defined as

$$\mathbf{x} = \zeta \circ \begin{bmatrix} a_{-N} \exp[j(\kappa p_{-N} + \pi\mu[N-\eta]^2)] \\ a_{-N+1} \exp[j(\kappa p_{-N+1} + \pi\mu[(-N+1)-\eta]^2)] \\ \vdots \\ a_{N-1} \exp[j(\kappa p_{N-1} + \pi\mu[(N-1)-\eta]^2)] \\ a_N \exp[^{j(\kappa p_N + \pi\mu[N-\eta]^2)}] \end{bmatrix} + \boldsymbol{\epsilon}. \tag{5}$$

We revisit the significance of the phase scaling factor introduced in (3). It has been determined that this value enables us to control the identity of the LFM noise waveform in a unique manner and that it is primarily used to improve the contribution of the random phase component. If randomizing the phase is not essential, the scaling factor can be throttled to fully preserve the quadratic phase. The scaling factor is chosen from a set of values $0 \le \kappa \le 1$.

We evaluate the ambiguity function of the LFM noise waveform as a function of time-delay and Doppler shift using the continuous-time equivalent of the LFM noise waveform. We define it as

$$\begin{aligned} \Omega(d, f_D) &= \int_{-\infty}^{\infty} v(t) v^*(t-d) e^{j2\pi f_D t} dt \\ &= P(t, f_D + \mu t) \end{aligned} \tag{6}$$

where $\Omega(d, f_D)$ is the notation used to represent the ambiguity function for the LFM noise waveform

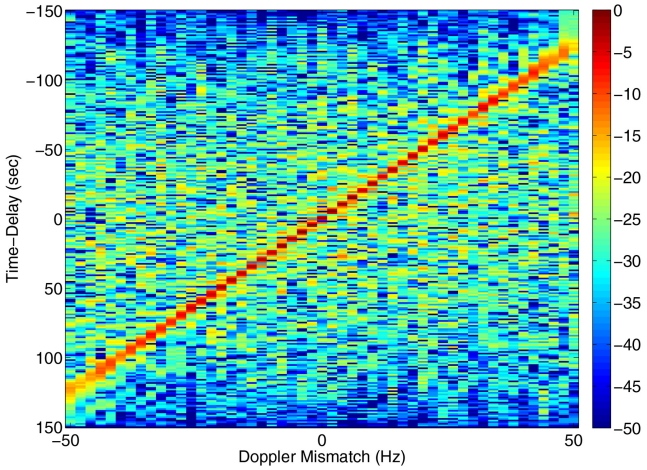

Fig. 1. Ambiguity function for LFM noise waveform having $\tau = 2$ μs, $\beta = 30$ MHz, and $\kappa = 0$.

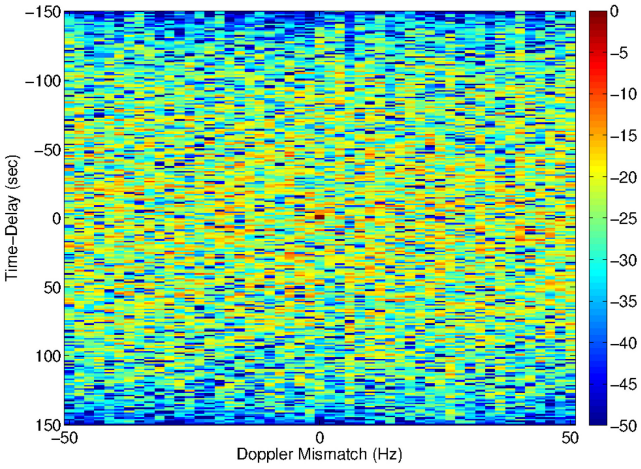

Fig. 2. Ambiguity function for LFM noise waveform having $\tau = 2$ μs, $\beta = 30$ MHz, and $\kappa = 1$.

and $P(d, f_D)$ is the classic chirp pulse ambiguity function [13].

By setting $\kappa = 0$, the random phase of the LFM noise waveform is removed such that $\mathbf{v} = \mathbf{a} \circ e^{j0\mathbf{p}} \circ \mathbf{s} \equiv \mathbf{a} \circ \mathbf{s}$. As a result the LFM noise waveform reduces to a nonconventional waveform that has random amplitude, but with Doppler tolerance comparable with a conventional chirp waveform. This is evident from Fig. 1, where the ambiguity function of the LFM noise waveform is similar to that of the conventional chirp [13]. When comparing these we notice the presence of a sloped ridge across the range-Doppler plane. The ridge represents the area of the matched filter output where target signal strengths will peak. The sloped nature suggests that the matched filter output will correlate with various delayed replicas despite range measurement error. Setting $\kappa = 0$ maximizes the ability of the LFM noise waveform to unambiguously resolve targets in range and Doppler.

By setting $\kappa = 1$, the random phase component of the LFM noise waveform is improved such that $\mathbf{v} = \mathbf{a} \circ e^{j1\mathbf{p}} \circ \mathbf{s} \equiv \mathbf{a} \circ \mathbf{p}$. As a result the peak output of the matched filter process lies at the center of the plot, and the LFM noise waveform behaves entirely like a random noise waveform where low probability of intercept (LPI) is achieved [13]. This is evident from Fig. 2, where the ambiguity function of the LFM noise waveform is a thumbtack and is only able to autocorrelate with zero-delayed replicas. Setting $\kappa = 1$ improves the random phase component, which maximizes the LPI and CCI-adverse characteristics of the LFM noise waveform [14].

By setting $\kappa = 0.5$, the phase of the LFM noise waveform is random but with a small enough variance to still preserve a partially quadratic shape. This is evident from Fig. 3, where the ambiguity function of the LFM noise waveform is similar to the chirp waveform [13]. Setting $\kappa = 0.5$ ensures some Doppler tolerance, LPI, and immunity to CCI [14]. As a result

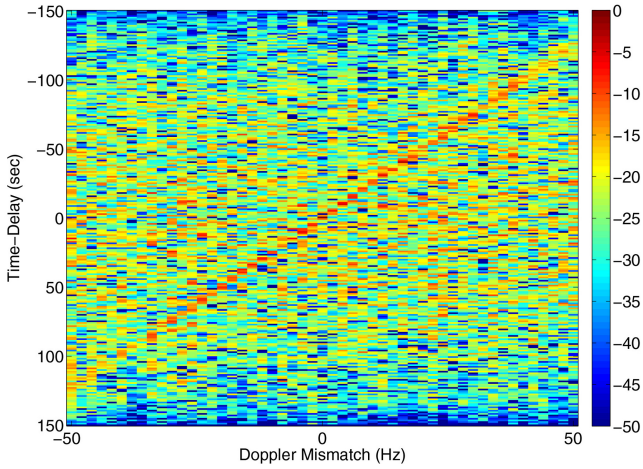

Fig. 3. Ambiguity function for LFM noise waveform having $\tau = 2$ μs, $\beta = 30$ MHz, and $\kappa = 0.5$.

the LFM noise waveform embodies characteristics from both the chirp and random noise waveforms.

III. ANALYSIS OF THE MATCHED FILTER OUTPUT

We analyze how well the LFM noise waveform can resolve targets. Results are compared with the chirp waveform. In our analysis we consider stationary targets for the first case and moving targets for the second. In both cases we assume a channel noise figure of 4 dB, a typical value for radar. We synthesize an array consisting of three targets staggered in range. The signal processing involves the analysis of the matched filter output using four popular radar sidelobe weighting functions [1]. For the stationary target case the times corresponding to positive initial range offsets are calculated by $2R_0/c$, and once quantized, they show up as negative shifts in the receive signal plus noise $x[n] = \zeta \cdot v[n - \eta] + \epsilon$. The range offsets chosen are $R_0 = [0, 50, 100]$ m, and their corresponding delays are calculated to be $[0, 0.33, 0.67]$ μs, respectively. Therefore, targets with

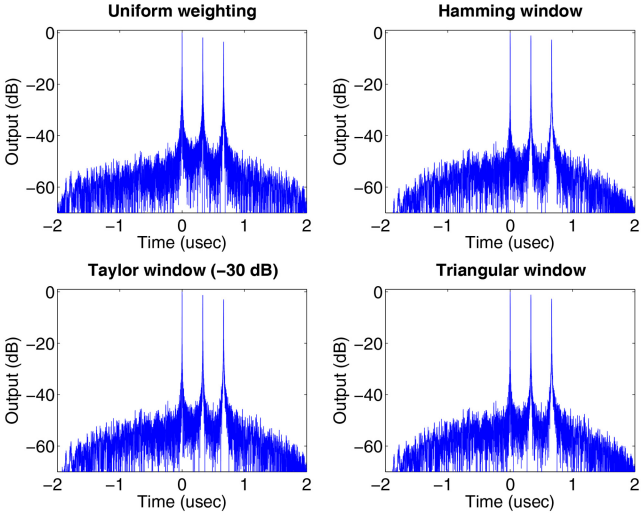

Fig. 4. Matched filter output of chirp waveform for three stationary targets having $\zeta = [5,5,5]$ m^2 and $R_0 = [0,50,100]$ m for $\tau\beta = 1500$.

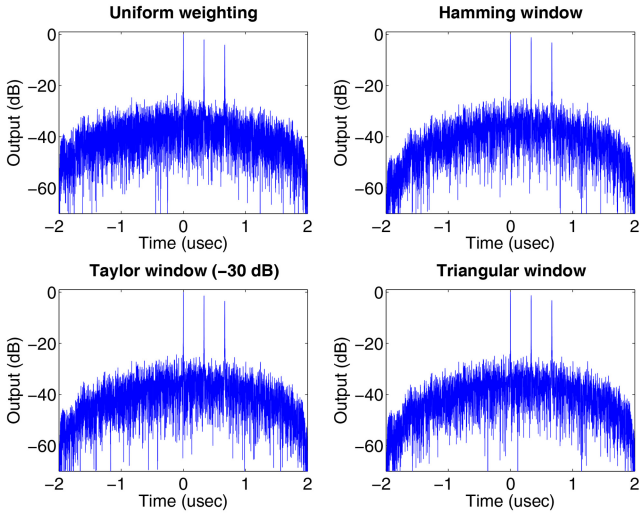

Fig. 5. Matched filter output of LFM noise waveform for three stationary targets having $\zeta = [5,5,5]$ m^2 and $R_0 = [0,50,100]$ m for $\tau\beta = 1500$. $\kappa = 0$.

sufficient peak-to-sidelobe level (PSL) are expected to exist at these times in the matched filter output.

The complementary subplots shown in the figures are of the matched filter output when different sidelobe weighting functions are used. The weighting functions were chosen based on common radar practice, and the intent for selecting these was to understand how different weighting functions could affect the matched filter output. The first window incorporates a uniform weighting ($w = 1$) and essentially imposes no weighting on the matched filter output. The other functions used are Hamming, Taylor (-30 dB PSL), and triangular [1].

Figure 4 plots the matched filter output for the chirp waveform for $\beta = 750$ MHz and $\tau = 2$ μs which equate to a time-bandwidth product of 1500. This figure is used as a reference. Typically, pulse compression ratios on the order of 10^3 are realized, but it is not uncommon to see ratios well in excess of this [1]. As evidenced by Fig. 4, three distinct targets are resolved at the calculated ranges (times).

Using the LFM noise waveform for the same time-bandwidth product and setting the phase scaling factor to $\kappa = 0$, we see, from Fig. 5, that the matched filter output is able to resolve and correctly range to the same three targets as the chirp despite marginal differences in PSL. Measurements of the matched filter output for a single target that has zero-time delay have been conducted [14]. Results from the experimental measurements quantified the sidelobe levels for each of the window functions considered in the simulation using different time-bandwidth products and κ values. It has been determined that uniform weighting offers the best PSL given moderate time-bandwidth products. As the time-bandwidth product increased, it was shown that the PSL for the remaining weighting functions converged to

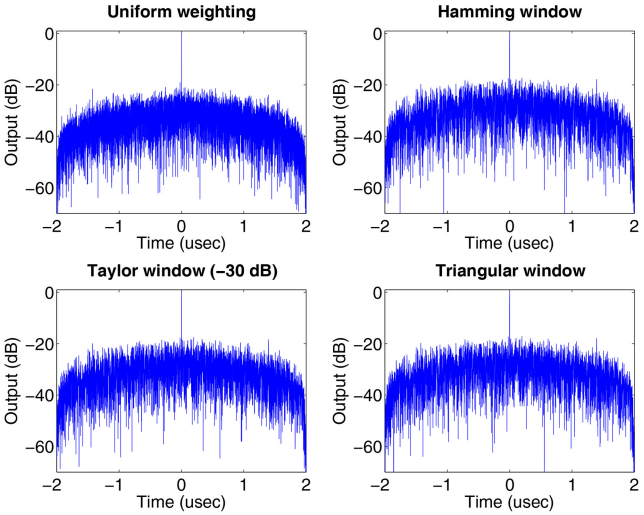

Fig. 6. Matched filter output of LFM noise waveform for three stationary targets having $\zeta = [5,5,5]$ m^2 and $R_0 = [0,50,100]$ m for $\tau\beta = 1500$. $\kappa = 1$.

that of the chirp, while the integrated sidelobe level (ISL) remained inferior regardless of increases to the time-bandwidth product.

Using the LFM noise waveform for the same time-bandwidth product and setting the phase scaling factor to $\kappa = 1$, we see, from Fig. 6, that the matched filter output is only able to resolve the zero-delayed target. This outcome is due to the fact that the phase is now completely random and that the LFM noise waveform is essentially identical to a random noise waveform. The correlator output of a random noise waveform with $d = 0$ is shown in Fig. 8. As expected correlation is only achieved for the target having no range offset ($d = 0$). As is the case with any analog random noise-based system, the receive process must be tuned to correlate with the delay commensurate with the particular range offset. This also applies to

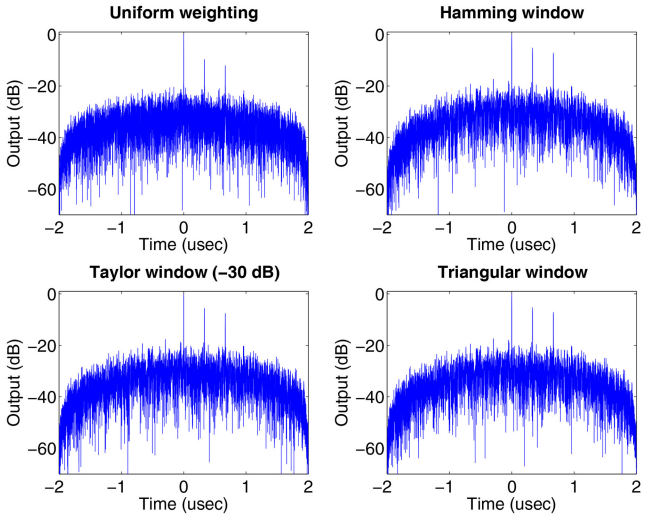

Fig. 7. Matched filter output of LFM noise waveform for three stationary targets having $\zeta = [5,5,5]$ m^2 and $R_0 = [0,50,100]$ m for $\tau\beta = 1500$. $\kappa = 0.5$.

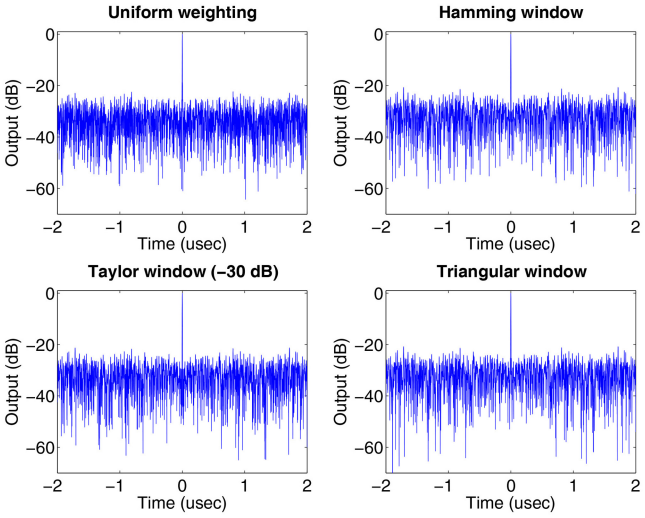

Fig. 8. Correlator output of random noise waveform having correlation delay = 0 for three moving targets having $\zeta = [5,5,5]$ m^2, $R_0 = [0,50,100]$ m, and $k_D = [0,750,1250]$.

Doppler shift. However, this can only be achieved for one target per processing interval. This limits practical moving target indication (MTI) applications and is certainly a disadvantage when compared with the conventional and LFM noise waveforms as illustrated in the previous example.

Using the LFM noise waveform for the same time-bandwidth product and setting the phase scaling factor to $\kappa = 0.5$, we see, from Fig. 7, that the matched filter output is still able to resolve and correctly range to the same three targets as the chirp. We notice that the PSL is less than the chirp and $\kappa = 0$ cases. This result is in agreement with the ambiguity function shown in Fig. 3. This reduction is due to the fact that the phase of the LFM noise waveform is partially randomized by the scaling factor. However, the phase scaling preserves a somewhat quadratic shape that allows the matched filter process to still resolve the target set.

The second case considers target movement and the resulting Doppler frequency effect that slowly displaces the target from its initial range. As time passes the movement of the target causes the measured range to change. By inspection of (6) the partial argument in $P(\cdot)$ is $f_D + \mu t$, which suggests that the Doppler will affectively add to the μt term. By normalizing this argument by μ, we can represent the result in the time domain and identify the expected delays when Doppler is present. Therefore, if we evaluate $(f_D/\mu) + t$ for positive Doppler cycles, $k_D = [0,750,1250]$, and consider the range-offsets from the stationary case where $t = [0,0.33,0.67]$ μs, we can determine the Doppler-shifted ranges (times) to be at $[0,-0.67,-1]$ μs, respectively.

Figure 9 plots the matched filter output for the chirp waveform that has a time-bandwidth product of 1500. We observe that the three targets are displaced

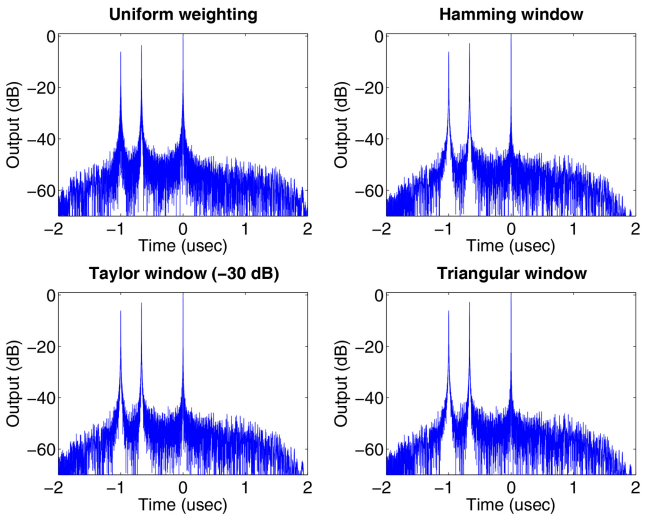

Fig. 9. Matched filter output of chirp waveform for three moving targets having $\zeta = [5,5,5]$ m^2, $R_0 = [0,50,100]$ m, $k_D = [0,750,1250]$ for $\tau\beta = 1500$.

to the calculated Doppler-shifted times. The outputs shown in Figs. 10–12 are compared with the chirp. It can be observed that the matched filter outputs for the LFM noise waveform with $\kappa = 0$ (Fig. 10) and $\kappa = 0.5$ (Fig. 12) are able to correctly resolve and range to the three moving targets. The $\kappa = 1$ case only correlates with the target that has zero range and Doppler offset ($d = 0$, $f_D = 0$). This result is expected and is in agreement with the ambiguity function shown in Fig. 2.

IV. CONCLUSIONS

We analyzed the range and Doppler resolution of an LFM noise radar waveform that had Rayleigh-distributed amplitude and uniform, evenly distributed phase. It has been determined that the value of the phase scaling factor directly affects

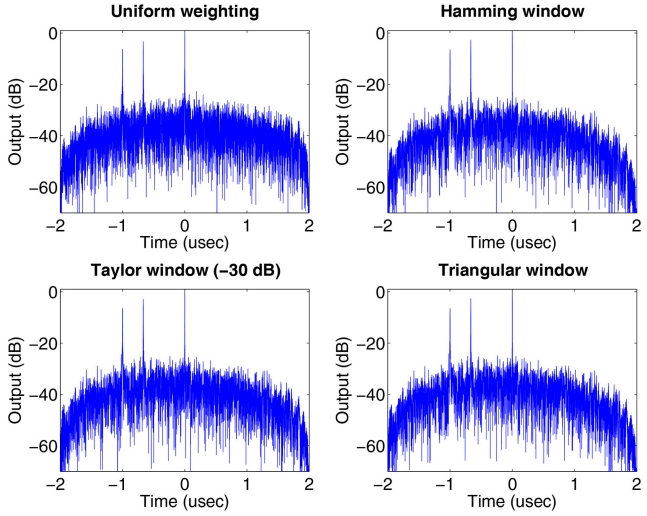

Fig. 10. Matched filter output of LFM noise waveform for three moving targets having $\zeta = [5,5,5]$ m^2, $R_0 = [0,50,100]$ m, $k_D = [0,750,1250]$ for $\tau\beta = 1500$. $\kappa = 0$.

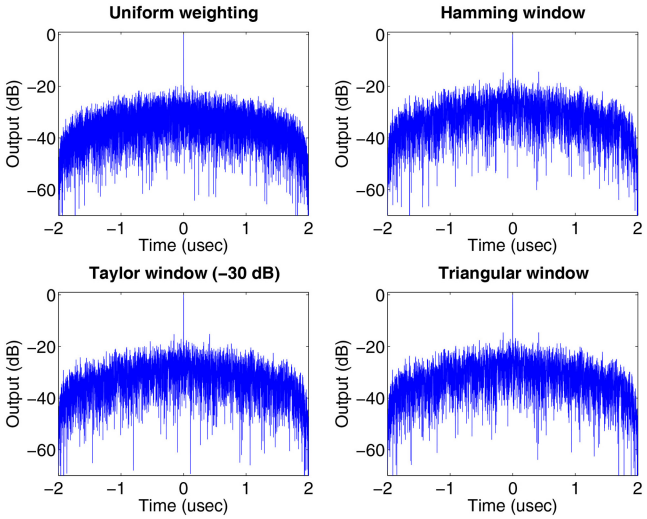

Fig. 11. Matched filter output of LFM noise waveform for three moving targets having $\zeta = [5,5,5]$ m^2, $R_0 = [0,50,100]$ m, $k_D = [0,750,1250]$ for $\tau\beta = 1500$. $\kappa = 1$.

the identity of the waveform in a unique manner. By selectively choosing the value of the scaling factor, one can ensure that the resulting waveform is optimized for the radar application.

Results from the radar ambiguity function suggest that we can maximize the Doppler tolerance of the LFM noise waveform by setting $\kappa = 0$. This would be ideal for an MTI application where security and the risk of CCI are not a precedent. Conversely, selecting $\kappa = 1$ maximizes the random phase contribution and results in a random noise waveform. This phase scaling factor would be warranted when the threat of interception and/or CCI is great. Lastly, we analyzed the radar ambiguity function when $\kappa = 0.5$ and observed that features from both the chirp and random noise waveforms were embodied in the output. By choosing $\kappa = 0.5$,

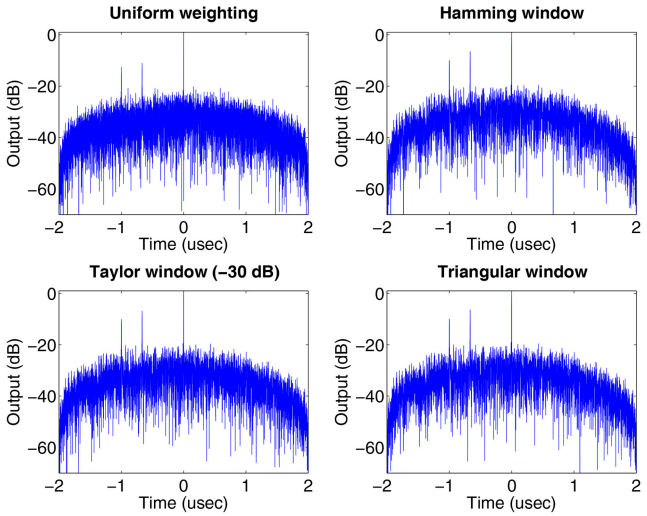

Fig. 12. Matched filter output of LFM noise waveform for three moving targets having $\zeta = [5,5,5]$ m^2, $R_0 = [0,50,100]$ m, $k_D = [0,750,1250]$ for $\tau\beta = 1500$. $\kappa = 0.5$.

the experimental simulation suggested the resulting waveform could serve as an LPI waveform for an MTI application.

Plots of the matched filter output demonstrated that the LFM noise waveform was able to resolve both stationary and moving targets with sufficient PSL. This fact is contingent on both the phase scaling factor and large time-bandwidth products. Results were in agreement with those of the radar ambiguity function, where it was shown that lower phase scaling factors result in optimal performance. Our inclusion of several conventional windows did not adversely affect the matched filter output and offered no processing advantages over uniform weighting for the given target set. It should be noted, however, that the matched filter for the LFM noise waveform is more sensitive to increases in channel noise and filter mismatch because of its inherently random nature. This could be an issue given physically smaller targets.

A select point not addressed in this paper pertains to the comparative analysis involving the LPI aspects of the LFM noise waveform in the presence of a passive listening device. With this in mind the LPI aspect of the LFM noise waveform can be substantiated. Furthermore, future research will focus on ways to adaptively select the appropriate phase scaling factor as a function of the operational environment.

MARK A. GOVONI
U.S. Army RDECOM CERDEC 12WD
Radar Application Branch
Building 6003
RDER-IWR-RA
Aberdeen Proving Ground
21005
E-mail: (mark.anthony.govoni@us.army.mil)

HONGBIN LI
Stevens Institute of Technology
Hoboken, NJ 07030

JOHN A. KOSINSKI[1]
Monmouth University
W. Long Branch, NJ 07764

[1]Also with MacAulay-Brown, Inc. Dayton, OH 45430

REFERENCES

[1] Skolnik, M.
Radar Handbook.
New York: McGraw-Hill, Jan. 2008, pp. 4.1–4.6.

[2] Guosui, L., et al.
The present and future of random signal radars.
IEEE Aerospace and Electronic Systems Magazine, **12**, 10 (Oct. 1997), 35–40.

[3] Narayanan, R. M. and Dawood, M.
Doppler estimation using a coherent ultrawide-band random noise radar.
IEEE Transactions on Antennas and Propagation, **48**, 6 (Jan. 2000), 868–878.

[4] Sun, H., Lu, Y., and Liu, G.
Ultra-wideband technology and random signal radar: An ideal combination.
IEEE Aerospace and Electronic Systems Magazine, **18**, 11 (Nov. 2003), 3–7.

[5] Axelsson, S.
Noise radar using random phase and frequency modulation.
Proceedings of the 2003 IEEE International Geoscience and Remote Sensing Symposium (IGARSS '03), vol. 7, Toulouse, France, July 21–25, 2003, pp. 4226–4231.

[6] Lukin, K. A., et al.
Implementation of software radar concept in surveillance radar on the basis of pulsed noise waveform.
Proceedings of the International Conference on the Noise Radar Technology (NRT 2003), Kharkov, Ukraine, Oct. 2003, pp. 15–16.

[7] Soumekh, M.
SAR-ECCM using phase-perturbed LFM chirp signals and DRFM repeat jammer penalization.
IEEE Transactions on Aerospace and Electronic Systems, **42**, 1 (Jan. 2006), 191–205.

[8] Kalinin, V., et al.
Ultra wideband wireless communication on the base of noise technology.
Proceedings of the International Conference on Microwaves, Radar & Wireless Communications (MIKON), Krakow, Poland, May 2006, pp. 615–618.

[9] Thayaparan, T., Dakovic, M., and Stankovic, L.
Mutual interference and low probability of interception capabilities of noise radar.
IET Radar, Sonar, and Navigation, **2**, 4 (2008), 294–305.

[10] Kulpa, K., Gajo, Z., and Malanowski, M.
Robustification of noise radar detection.
IET Radar, Sonar & Navigation, **2**, 4 (2008), 284–293.

[11] Lukin, K. A.
Noise radar technology: The principles and short overview.
Applied Radio Electronics, **4**, 1 (2005), 4–13.

[12] Li, Z. and Narayanan, R. M.
Doppler visibility of coherent ultrawideband random noise radar system.
IEEE Transactions on Aerospace and Electronics, **42**, 3 (July 2006), 904–916.

[13] Richards, M.
Fundamentals of Radar Signal Processing.
New York: McGraw-Hill, Jan. 2005, pp. 188–198.

[14] Govoni, M. A.
Linear frequency modulation of stochastic radar waveform.
Ph.D. dissertation, Stevens Institute of Technology, Hoboken, NJ, Apr. 2011.